Dynamic Bayesian Networks for Vehicle Classification in Video

Mehran Kafai, *Student Member, IEEE*, and Bir Bhanu, *Fellow, IEEE*

***Abstract*—Vehicle classification has evolved into a significant subject of study due to its importance in autonomous navigation, traffic analysis, surveillance and security systems, and transportation management. While numerous approaches have been introduced for this purpose, no specific study has been conducted to provide a robust and complete video-based vehicle classification system based on the rear-side view where the camera's field of view is directly behind the vehicle. In this paper, we present a stochastic multiclass vehicle classification system which classifies a vehicle (given its direct rear-side view) into one of four classes: sedan, pickup truck, SUV/minivan, and unknown. A feature set of tail light and vehicle dimensions is extracted which feeds a feature selection algorithm to define a low-dimensional feature vector. The feature vector is then processed by a hybrid dynamic Bayesian network to classify each vehicle. Results are shown on a database of 169 videos for four classes.**

***Index Terms*—Classification, hybrid dynamic Bayesian network (HDBN).**

I. Introduction

OVER THE past few years, vehicle classification has been widely studied as part of the broader vehicle recognition research area. A vehicle classification system is essential for effective transportation systems (e.g., traffic management and toll systems), parking optimization, law enforcement, autonomous navigation, etc. A common approach utilizes vision-based methods and employs external physical features to detect and classify a vehicle in still images and video streams. A human being may be capable of identifying the class of a vehicle with a quick glance at the digital data (image, video) but accomplishing that with a computer is not as straight forward. Several problems such as occlusion, tracking a moving object, shadows, rotation, lack of color invariance, and many more must be carefully considered in order to design an effective and robust automatic vehicle classification system which can work in real-world conditions.

Manuscript received April 30, 2011; revised August 19, 2011; accepted October 09, 2011. Date of publication October 21, 2011; date of current version January 20, 2012. This work was supported in part by National Science Foundation under Grant 0905671. The content of the information does not reflect the position or policy of the U.S. Government. Paper no. TII-11-240.

M. Kafai is with the Center for Research in Intelligent Systems, Computer Science Department, University of California, Riverside, CA 92521 USA (e-mail: mkafai@cs.ucr.edu).

B. Bhanu is with the Center for Research in Intelligent Systems, University of California, Riverside, Riverside, CA 92521 USA (e-mail: bhanu@cris.ucr.edu).

Color versions of one or more of the figures in this paper are available online at http://ieeexplore.ieee.org.

Digital Object Identifier 10.1109/TII.2011.2173203

Feature-based methods are commonly used for object classification. As an example, scale invariant feature transform (SIFT) represents a well-studied feature-based method. Using SIFT, an image is represented by a set of relatively invariant local features. SIFT provides pose invariance by aligning features to the local dominant orientation and centering features at scale space maxima. It also provides appearance change resilience and local deformation resilience. To the contrary, reliable feature extraction is limited when dealing with low resolution images in the real-world conditions.

Much research has been conducted for object classification, but vehicle classification has shown to have its own specific problems which motivates research in this area.

In this paper, we propose a hybrid dynamic Bayesian network (HDBN) as part of a multiclass vehicle classification system which classifies a vehicle (given its direct rear-side view) into one of four classes: sedan, pickup truck, SUV/minivan, and unknown. High resolution and closeup images of the logo, license plate, and rear view are not required due to the use of simple low-level features (e.g., height, width, and angle) which are also computationally inexpensive.

In the rest of this paper, Section II describes the related work and contributions of this study. Section III discusses the technical approach and system framework steps. Section IV explains the data collection process and shows the experimental results. Finally, Section V concludes this paper.

II. Related Work and Our Contributions

A. Related Work

Not much has been done on vehicle classification from the rear view. For the side view, appearance-based methods especially edge-based methods have been widely used for vehicle classification. These approaches utilize various methods such as weighted edge matching [1], Gabor features [2], edge models [3], shape-based classifiers, part based modeling, and edge point groups [4]. Model-based approaches that use additional prior shape information have also been investigated in 2-D [5] and more recently in 3-D [6], [7].

Shan *et al.* [1] presented an edge-based method for vehicle matching for images from nonoverlapping cameras. This feature-based method computed the probability of two vehicles from two cameras being similar. The authors define the vehicle matching problem as a two-class classification problem, thereafter apply a weak classification algorithm to obtain labeled samples for each class. The main classifier is trained by a unsupervised learning algorithm built on Gibbs sampling and

TABLE I
RELATED WORK SUMMARY

Author	Principles & Methodology
Psyllos *et al.* [10]	frontal view, neural network classification, Phase congruency calculation, SIFT fingerprinting
Conos *et al.* [9]	frontal view, kNN classifier, SIFT descriptors, frontal view images
Chen *et al.* [12]	side view, multi-class SVM classifier, color histograms
Zhang *et al.* [13]	side view, shape features, wavelet fractal signatures, fuzzy k-means
Shan *et al.* [1]	side view, edge-based, binary classification, Fishers Linear Discriminants, Gibbs sampling, unsupervised learning
Wu *et al.* [3]	side view, neural network classification, parametric model
This Paper	rear view, Hybrid Dynamic Bayesian Network

Fisher's linear discriminant using the labeled samples. A key limitation of this algorithm is that it can only perform on images that contain similar vehicle pose and size across multiple cameras.

Wu *et al.* [3] use a parameterized model to describe vehicle features, thenceforth embrace a multilayer perceptron network for classification. The authors state that their method falls short when performing on noisy and low-quality images and that the range in which the vehicle appears is small.

Wu and Zhang [8] propose a principal component analysis (PCA)-based classifier where a subspace is inferred for each class using PCA. As a new query sample appears, it is projected onto all class subspaces and is classified based on which projection results in smaller residue or truncation errors. This method is used for multiclass vehicle classification for static road images. Experiments show that it has better performance compared to linear support vector machine (SVM) and Fisher linear discriminant.

Vehicle make and model recognition from the frontal view is investigated in [9] and more recently in [10]. Psyllos *et al.* [10] use closeup frontal view images and a neural network classifier to recognize the logo, manufacturer, and model of a vehicle. The logo is initially segmented and then used to recognize the manufacturer of the vehicle. The authors report 85% correct recognition rate for manufacturer classification and only 54% for model recognition. Such an approach entirely depends on the logo; therefore, it might fail if used for the rear view as the logo may not always be present.

For the rear view, Dlagnekov and Belongie [11] develop a vehicle make and model recognition system for video surveillance using a database of partial license plate and vehicle visual description data, and they report a recognition accuracy of 89.5%. Visual features are extracted using two feature-based methods (SIFT and shape context matching) and one appearance-based method (Eigencars). The drawbacks of the proposed system are that it is relatively slow, and only the license plate recognition stage is done in real-time.

A summary of related work is shown in Table I.

For the side view, we have conducted a study for vehicle recognition using pseudotime series. After some preprocessing (moving vehicle detection, shadow removal) and automatically tracing the boundary pixels, the vehicle 2-D blob shape is converted to a pseudotime series using either radius distance scanning or local neighborhood curvature. Fig. 1(b) and (c) demonstrates the time series representing the sample vehicle boundary in Fig. 1(a).

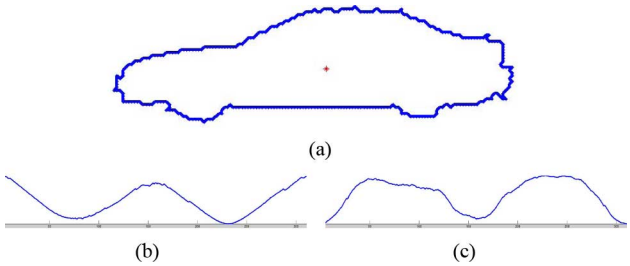

Fig. 1. Converting vehicle boundary shape into time series. (a) Vehicle boundary. (b) Resulting time series using radius distance. (c) Resulting time series using local neighborhood curvature.

Fig. 2. Sample images of the direct rear view of a moving vehicle.

Pseudotime series works well for side-view vehicle classification (see Section IV-A) but will not perform as well if used for frontal view or rear view due to boundary shape similarity.

B. Contributions of This Paper

Unlike the previous work, as shown in Table I, the contributions of this paper are the following.

1) We propose a probabilistic classification framework which determines the class of a vehicle given its direct rear view (see Fig. 2). We choose the direct rear view for two main reasons. First, most of the research in this area has focused on the side view (see [1]–[3]), whereas the frontal view and rear view have been less investigated. Second, not all states require a front license plate (19 states in the U.S. require only the rear license plate). We introduce an HDBN classifier with multiple time slices corresponding to multiple video frames.
2) We eliminate the need for high resolution and closeup images of the logo, license plate, and rear view by using simple low-level features (e.g., height, width, and angle) which are also computationally inexpensive; thus, the proposed method is capable of running in real time.
3) The results are shown on a database of 169 real videos consisting of sedan, pickup truck, SUV/minivan, and also a class for unknown vehicles.

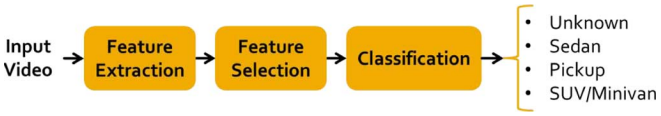

Fig. 3. System framework.

We adapt, modify, and integrate computational techniques to solve a new problem that has not been addressed or solved by anyone. Vehicle classification has been investigated by many people. The novelty of our work comes from using the HDBN classifier for rear-view vehicle classification in video. Our approach is a solution to important practical applications used in law enforcement, parking security, etc. For example, when a vehicle is parked in a parking lot, the rear view is usually visible and the frontal-view and side-view images cannot be captured. In this case, rear-view classification is essential for parking lot security and management.

The key aspects of our paper are as follows.

1) A novel structure for the HDBN is proposed, specifically designed to solve a practical problem. The HDBN classifier has never before been used in the context of proposed video application. Rear-side view classification has not been studied in video.
2) The HDBN is defined and structured in a way that adding more rear view features is easy, missing features that were not extracted correctly in one or more frames of a video are inferred in the HDBN and, therefore, classification does not completely fail.
3) A complete system including feature extraction, feature selection, and classification is introduced with significant experimental results.

III. Technical Approach

The complete proposed system pipeline is shown in Fig. 3. All components are explained in the following sections.

A. Feature Extraction

Three main types of features are extracted from the images: tail lights, license plate, and rear dimensions. The tail light features include separately for each tail light the width, distance from the license plate, and angle between tail light and license plate. The license plate location and size is used as a reference to enable comparison and help normalize tail light properties and vehicle size values. The feature extraction component consists of three subcomponents: vehicle detection, license plate extraction, and tail light extraction.

1) Vehicle Detection: Object detection is an active research topic in transportation systems (see [14]–[17]). In this paper, a Gaussian mixture model approach is used for moving object detection. The Gaussian distributions are used to determine if a pixel is more likely to belong to the background model or not. An AND approach is used which determines a pixel as background only if it falls within three standard deviations for all the components in all three R, G, and B color channels [18]. We validate the detected moving object by using a simple frame differencing approach and cross checking the masks from both methods.

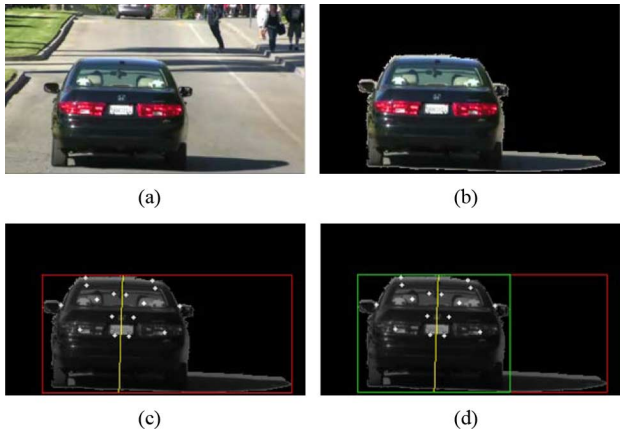

Fig. 4. Shadow removal and obtaining the bounding box. (a) Original image. (b) Moving object mask. (c) Initial bounding box. (d) Readjusted bounding box.

The resulting mask may include some shadow and erroneous pixels. The shadow is removed by finding the vertical axis of symmetry using an accelerated version of Loy's symmetry [19] and readjusting the bounding box containing the mask with respect to the axis of symmetry. This is done by measuring the distance between each point on both vertical sides of the bounding box and the axis symmetry and moving the vertical side that is farther away closer to the axis of symmetry such that each side has the same distance from it. Fig. 4 shows results from multiple steps of this approach. The aforementioned shadow removal method fails if the shadow is behind the vehicle. In such cases, the shadow is removed using the approach introduced by Nadimi and Bhanu [20] which does not rely on the common geometrical assumptions such as camera location, object geometry, and ground surface geometry. Given the vehicle rear mask, the height and width of the bounding box and area of the mask are measured.

2) License Plate Extraction: We use the license plate corner coordinates as input to our algorithm. There are number of algorithms for license plate extraction (see [21], [22]). Anagnostopoulo *et al.* [22] propose using sliding concentric window segmentation, masking, and Sauvola binarization to identify the license plate location. They report a 96.5% success rate on a database of 1334 images.

In this paper, we have focused on novel aspects of HDBN classifier and the integrated system. This allows us to quantify the results at the system level independent of the particular algorithm used for license plate extraction. We have described a license detection approach in Sections III-A2a. The classification results are obtained by manual license plate detection. However, the proposed or any other license detection algorithm can be easily integrated into our system.

a) Automatic License Plate Extraction: The license plate is extracted using two separate methods and then the "best" result is chosen. The first method is proposed by Abolghasemi and Ahmadyfard [23], where a matched filtering approach is applied to extract candidate plate-like regions. The contrast of plate-like

Fig. 5. License plate extraction.

Fig. 6. Tail light detection.

regions is enhanced using vertical edge density, and detection is performed using colored texture in the plate.

In addition to the method from [23], we apply a blob detection and filtering method to improve license plate detection. This additional method consists of the following steps.

1) Detect edges.
2) Generate binary image with selectable blobs. Image is processed to accent the more apparent detected edges and to fill and smooth the image where appropriate.
3) Determine the blob that most likely corresponds to the license plate. In a cascading form, filter the blobs using the following attributes: blobs with a side length comparable to a license plate, blobs that are horizontally aligned, blob size relative to a license plate, squareness of blob, blobs that are far too linear in shape, closest ideal area, and closest total distance to the centroid from multiple points.

The result from the method of vertical edge detection and match filtering is compared with the result from the method of blob detection and match filtering.

Both methods are given a score on which solution is most likely the actual license plate. The scoring systems awards points for the following attributes: accurate license plate to bounding box ratios, the centering of the license plate returned across the axis of symmetry, how equal the centering on the axis of symmetry is, prediction of each side in comparison to the centroid, the average color of the license plate, and the squareness presented by both solutions. The solution with the highest score value is then selected as the most accurate prediction of the license plate location. Fig. 5 shows some results of the license plate extraction component. The overall license plate extraction rate is 98.2% on a dataset of 845 images. The extracted license plate height and width measurements for 93.5% of the dataset have $\pm 15\%$ error compared to the actual license plate dimensions, and 4.7% have between $\pm 15\%$ and $\pm 30\%$ error.

3) Tail Light Extraction: For tail light detection the regions of the image where red color pixels are dominant are located. We compute the redness of each image pixel by fusing two methods. In the first approach [24], the image is converted to HSV (Hue, Saturation, Value) color space and then pixels are classified into three main color groups red, green, and blue. The second method proposed by Gao and Correia [25] defines the red level of each pixel as $r_i = 2R_i/G_i + B_i$ in RGB color space. A bounding box surrounding each tail light is generated by combining results from both methods and checking if the regions with high redness can be a tail light (e.g., are symmetric and are close to the edges of the vehicle). Fig. 6 presents results of the two methods and the combined result as two bounding boxes. Both these methods fail if the vehicle body color is red itself. To overcome this, the vehicle color is estimated using an HSV color space histogram analysis approach which determines if the vehicle is red or not. If a red vehicle is detected, the tail light detection component is enhanced by adding an extra level of postprocessing which includes Otsu's thresholding [26], color segmentation, removing large and small regions, and symmetry analysis. After the tail lights are detected, the width, centroid, and distance and angle with the license plate are separately computed for both left and right tail lights.

Tail light detection is challenging for red vehicles. Our approach performs well considering the different components involved (symmetry analysis, size filtering, thresholding, etc.). However, for more accurate tail light extraction, Otsu's method may not be sufficient. For our future work, we plan to consider more sophisticated methods such as using physical models [20] to distinguish the lights from the body based on the characteristics of the material of a vehicle.

4) Feature Set: As the result of the feature extraction component the following 11 features are extracted from each image frame (all distances are normalized with respect to the license plate width):

1) perpendicular distance from license plate centroid to a line connecting two tail light centroids;
2) right tail light width;
3) left tail light width;
4) right tail light-license plate angle;
5) left tail light-license plate angle;
6) right tail light-license plate distance;
7) left tail light-license plate distance;
8) bounding box width;
9) bounding box height;
10) license plate distance to bounding box bottom side;
11) vehicle mask area.

A vehicle may have a symmetric structure but we chose to have separate features for the left side and right side so that the classifier does not completely fail if during feature extraction a feature (e.g., tail light) on one side is not extracted accurately. Also, the tail light-license plate angles may differ for the left and right side because the license plate may not be located in the center exactly.

B. Feature Selection

Given a set of features Y, feature selection determines a subset X which optimizes an evaluation criterion J. Feature selection is performed for various reasons including improving classification accuracy, shortening computational time, reducing measurements costs, and relieving the curse of dimensionality. We chose to use sequential floating forward

selection (SFFS), a deterministic statistical pattern recognition feature selection method which returns a single suboptimal solution. SFFS starts from an empty set and adds the most significant features (e.g., features that increase accuracy the most). It provides a kind of back tracking by removing the least significant feature during the third step, conditional exclusion. A stopping condition is required to halt the SFFS algorithm; therefore, we limit the number of feature selection iterative steps to 2^{n-1} (n is the number of features) and also define a correct classification rate (CCR) threshold of $b\%$, where b is greater than the CCR of the case when all features are used. In other words, the algorithm stops when either the CCR is greater than $b\%$, or 2^{n-1} iterations are completed. In the following, the pseudocode for SFFS is shown (k is the number of features already selected).

1) Initialization: $k = 0$; $X_0 = \{\emptyset\}$.
2) Inclusion: add the most significant feature

$$x_{k+1} = \arg\max_{x \in (Y - X_k)}[J(X_k + x)]$$
$$X_{k+1} = X_k + x_{k+1};\ \text{repeat step 2 if } k < 2.$$

3) Conditional exclusion: find the least significant feature and remove (if not last added)

$$x_r = \arg\max_{x \in X_k}[J(X_k - x)]$$
$$\text{if } x_r = x_{k+1} \text{ then } k = k + 1;\ \text{Go to step 1}$$
$$\text{else } X'_k = X_{k+1} - x_r.$$

4) Continuation of conditional exclusion

$$x_s = \arg\max_{x \in X'_k}[J(X'_k - x)]$$
$$\text{if } J(X'_k - x_s) \le J(X_{k-1}) \text{ then}$$
$$X_k = X'_k;\ \text{Go to step 2}$$
$$\text{else } X'_{k-1} = X'_k - x_s;\ k = k - 1.$$

5) Stopping condition check

$$\text{if } halt\_condition = true \text{ then STOP}$$
$$\text{else Go to step 4.}$$

Fig. 7 presents the CCR plot with feature selection steps as the x axis and CCR as the y axis. The plot peaks at $x = 5$ and the algorithm returns features 1, 4, 6, 10, and 11 as the suboptimal solution.

C. Classification

1) Known or Unknown Class: The classification component consists of a two stage approach. Initially, the vehicle feature vector is classified as known or unknown. To do such, we estimate the Gaussian distribution parameters of the distance to the nearest neighbor for all vehicles in the training dataset. To determine if a vehicle test case is known or unknown, first the distance to its nearest neighbor is computed. Then, following the empirical rule if the distance does not lie within four standard deviations of the mean ($\mu \pm 4\sigma$), it is classified as unknown. If the vehicle is classified as known, it is a candidate for the second stage of classification.

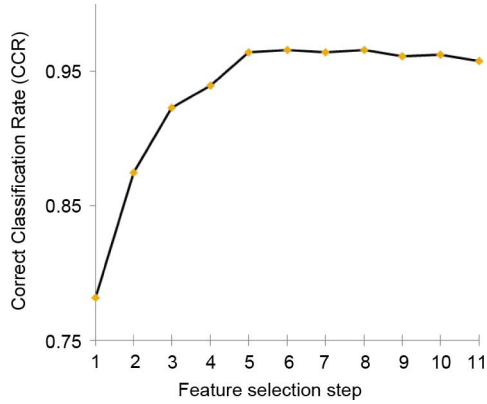

Fig. 7. Feature selection subset CCR plot.

2) Dynamic Bayesian Network for Classification: We propose to use dynamic Bayesian networks (DBNs) for vehicle classification in video. Bayesian networks offer a very effective way to represent and factor joint probability distributions in a graphical manner which makes them suitable for classification purposes. A Bayesian network is defined as a directed acyclic graph $G = (V, E)$, where the nodes (vertices) represent random variables from the domain of interest and the arcs (edges) symbolize the direct dependences between the random variables. For a Bayesian network with n nodes $X_1, X_2, \ldots, X_n$, the full joint distribution is defined as

$$\begin{aligned} p(x_1, x_2, \ldots, x_n) &= p(x_1) \times p(x_2|x_1) \times \cdots \\ &\quad \times p(x_n|x_1, x_2, \ldots, x_{n-1}) \\ &= \prod_{i=1}^{n} p(x_i|x_1, \ldots, x_{i-1}) \end{aligned} \tag{1}$$

but a node in a Bayesian network is only conditional on its parent's values; so

$$p(x_1, x_2, \ldots, x_n) = \prod_{i=1}^{n} p(x_i|parents(X_i)) \tag{2}$$

where $p(x_1, x_2, \ldots, x_n)$ is an abbreviation for $p(X_1 = x_1 \wedge \cdots \wedge X_n = x_n)$. In other words, a Bayesian network models a probability distribution if each variable is conditionally independent of all its nondescendants in the graph given the value of its parents.

The structure of a Bayesian network is crucial in how accurate the model is. Learning the best structure/topology for a Bayesian network takes exponential time because the numbers of possible structures for a set of given nodes is superexponential in the number of nodes. To avoid performing exhaustive search, we use the K2 algorithm (Cooper and Herskovits, 1992) to determine a suboptimal structure. K2 is a greedy algorithm that incrementally add parents to a node according to a score function. In this paper, we use the Bayesian information

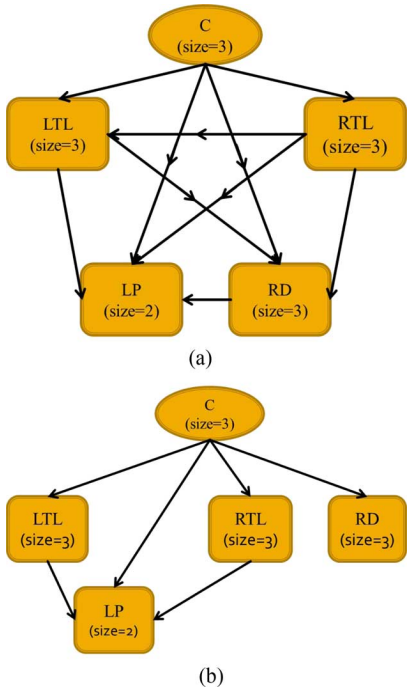

Fig. 8. Bayesian network structures. (a) K2 generated structure. (b) Manually structured Bayesian network.

criterion (BIC) function as the scoring function. Fig. 8(a) illustrates the resulting Bayesian network structure. We also define our manually structured network [see Fig. 8(b)] and we compare the two structures in Section IV-E. The details for each node are as follows.

1) C: vehicle class, discrete hidden node, size=3.
2) LP: license plate, continuous observed node, size=2.
3) LTL: left tail light, continuous observed node, size=3.
4) RTL: right tail light, continuous observed node, size=3.
5) RD: rear dimensions, continuous observed node, size=3.

For continuous nodes, the size indicates the number of features each node is representing, and for the discrete node C, it denotes the number of classes. RTL and LTL are continuous nodes and each contain the normalized width, angle with the license plate, and normalized Euclidean distance with the license plate centroid. LP is a continuous node with distance to the bounding box bottom side and perpendicular distance to the line connecting the two tail light centroids as its features. RD is a continuous node with bounding box width and height, and vehicle mask area as its features. For each continuous node of size n, we define a multivariate Gaussian conditional probability distribution, where each feature of each continuous node has $\mu = [\mu_1 \cdots \mu_n]^T$ and Σ as an $n \times n$ symmetric, positive-definite covariance matrix. The discrete node C has a corresponding conditional probability table assigned to it which defines the probabilities $P(C = sedan)$, $P(C = pickup)$, and $P(C = SUV\ or\ minivan)$.

Adding a temporal dimension to a standard Bayesian network creates a DBN. The time dimension is explicit, discrete, and helps model a probability distribution over a time-invariant process. In simpler words, a DBN is created by replicating a Bayesian network with time-dependent random variables over T time slices. A new set of arcs defining the transition model is also used to determine how various random variables are related between time slices. We model our video-based classifier by extending the aforementioned Bayesian network [see Fig. 8(b)] to a DBN. The DBN structure is defined as follows.

1) For each time slice $t_{i,i=1,2,...,5}$, the DBN structure is similar to the Bayesian network structure given in Fig. 8(b).
2) Each feature X_i^t is the parent of X_i^{t+1}.
3) C^t is the parent of C^{t+1}.
4) All intra slice dependencies (arcs) also hold as inter time slices except for arcs from time slice t hidden nodes to time slice $t+1$ observed nodes.

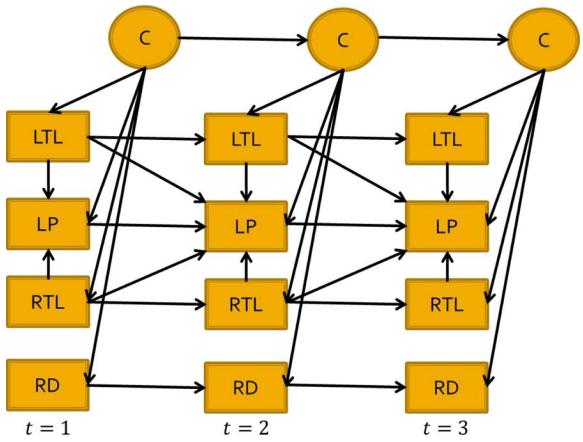

Fig. 9. DBN structure for time slices $t_{i,i=1,2,3}$.

Fig. 9 demonstrates the DBN structure for three time slices. Such a network is identified as an HDBN because it consists of discrete and continuous nodes. Training the HDBN or in other words learning the parameters of the HDBN is required before classification is performed. Therefore, the probability distribution for each node given its parents should be determined. For time slice t_1, this includes $p(LTL|C)$, $p(RTL|C)$, $p(RD|C)$, $p(LP|C, LTL, RTL)$, and $p(C)$. For time slices $t_{i,i=2,...,5}$, it includes

$$\begin{aligned} &p(LTL^t|C^t, LTL^{t-1}),\ p(RTL^t|C^t, RTL^{t-1}) \\ &p(C^t|C^{t-1}),\ p(RD^t|C^t, RD^{t-1}) \\ &p(LP^t|C^t, LTL^t, RTL^t, LP^{t-1}, LTL^{t-1}, RTL^{t-1}). \end{aligned} \quad (3)$$

For example, to determine $p(LTL^t|C^t, LTL^{t-1})$, three distributions with different parameters, one for each value of C^t, are required. Hence, $p(LTL^t|LTL^{t-1}, C^t = sedan)$, $p(LTL^t|LTL^{t-1}, C^t = pickup)$, and $p(LTL^t|LTL^{t-1}, C^t = SUV\ or\ Minivan)$ are estimated, and $p(LTL^t|LTL^{t-1})$ is derived by summing over all the C^t cases.

The next step is inference where a probability distribution over the set of vehicle classes is assigned to the feature vector representing a vehicle. In other words, inference provides $p(C^t|f^{(1:t)})$, where $f^{(1:t)}$ refers to all features from time slice t_1 to t_5.

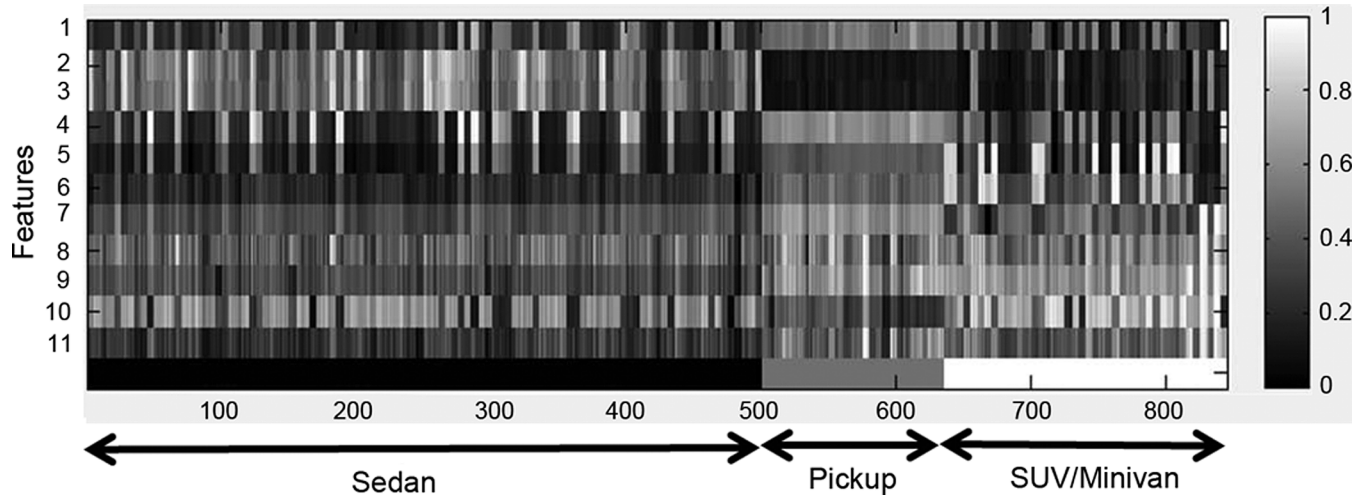

Fig. 10. Pattern-feature matrix for different vehicles.

TABLE II
CONFUSION MATRIX

Predicted Class →	Sedan	Pickup	Minivan	SUV
Sedan	30	0	0	0
Pickup	0	30	0	0
Minivan	0	0	28	2
SUV	2	1	2	25

IV. EXPERIMENTAL RESULTS

A. Side-View Vehicle Recognition

Our initial experiments are performed on a dataset consisting of 120 vehicles. The dataset includes four vehicle classes: sedan, pickup truck, minivan, and SUV, each containing 30 vehicles. We use dynamic time warping [27] to compute the distance, nearest neighbor for classification, and k-fold cross validation with $k = 10$ to evaluate our approach. The resulting confusion matrix is shown in Table II. The presented results are obtained by using radius distance time series as described earlier. We performed similar experiments using local neighborhood curvature and found similar results which are not shown here.

B. Rear-View Data Collection

We collected video data of passing vehicles using a Sony HDR-SR12 video camera. The videos are taken in the early afternoon with sunny and partly cloudy conditions. Lossless compressed PNG image files are extracted from the original HD MPEG4 AVC/H.264 video format, then downsampled from 1440×1080 to 320×240 using bicubic interpolation. Downsampling is performed to reduce the computation time. All image frames were manually labeled with the vehicle class to provide the ground truth for evaluation purposes. Fig. 11 shows three examples for each known vehicle class. The number in front of the class label denotes the difficulty level of classifying that case (e.g., Sedan 3 [see Fig. 11(c)] is harder to classify than Sedan 1 [see Fig. 11(a)]).

The dataset consists of 100 sedans, 27 pickup trucks, and 42 SUV/minivans. We have not added more SUV and pickup images to the database because the current number of samples for each class in the database reflects the actual distribution of vehicle classes at our data capture location. Before extracting the features and generating the feature set, it is important to determine the number of frames required for classification. We recorded classification accuracy for different number of frames. The maximum accuracy is achieved when five frames are used. Note that these frames are not successive. We are using $\Delta t = 2$ which means leaving out two frames between candidate frames. This value is directly related to the speed of the vehicle and the overall time the vehicle is visible in the camera's field of view. Although currently a predetermined value is used for Δt, we plan to automatically determine the optimal value as part of future work.

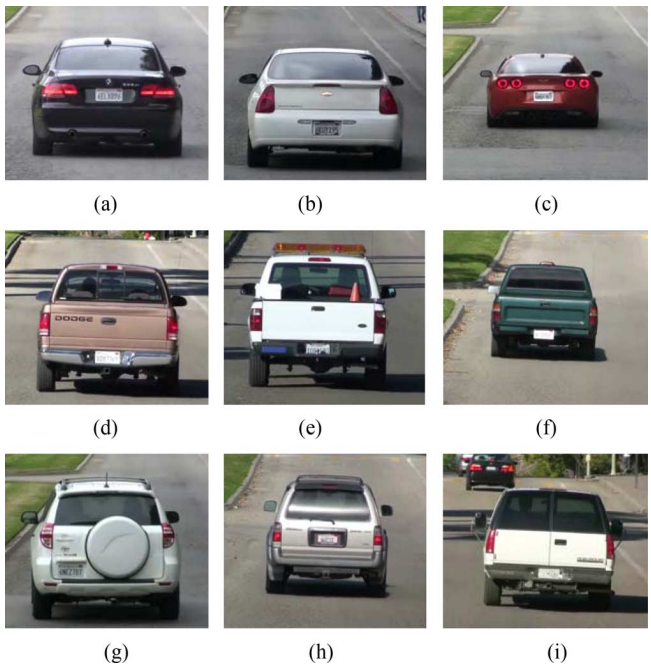

Fig. 11. Known vehicle examples for each class. (a) Sedan 1. (b) Sedan 2. (c) Sedan 3. (d) Pickup 1. (e) Pickup 2. (f) Pickup 3. (g) SUV 1. (h) SUV 2. (i) SUV 3.

Fig. 12. Unknown vehicle examples.

TABLE III
FEATURE SELECTION RESULTS

FS Method↓	Selected features	Precision	FA Rate	CCR	Testing time(s)
(a) None	all	95.68	0.02	97.63	0.05
(b) SFFS	1,4,6,10,11	94.23	0.03	96.68	0.03

TABLE IV
CONFUSION MATRIX

Pred. Class → True Class↓	Unknown	Sedan	Pickup	SUV/ Minivan	Total
Unknown	8	0	0	0	8
Sedan	0	99	1	0	100
Pickup	0	0	27	0	27
SUV/Minivan	0	3	2	37	42

To evaluate how well the algorithm performs in the case of an unknown vehicle, we also collected eight unknown vehicles which are not part of the training dataset. Fig. 12 shows two examples of unknown vehicles.

Fig. 10 shows the corresponding pattern-feature matrix. The y axis represents the extracted features and the x axis symbolizes all 845 (169 vehicles $\times 5$ frames) feature vectors. For presentation purposes, each row has been normalized by dividing by the maximum value of the same feature.

C. Feature Selection Evaluation

Table III shows classification evaluation metrics both when (a) using the entire feature set, and (b) using a suboptimal subset. Results show that using the subset of the features generated by SFFS decreases the accuracy and precision by approximately 1%. Feature selection also decreases the average testing time per frame from 0.05 to 0.03 s. The selected feature numbering is according to the features listed in Section III-A4.

D. Classification Results

We use the Bayes Net Toolbox [28], an open-source MATLAB package, for defining the DBN structure, parameter learning, and computing the marginal distribution on the class node. The proposed classification system was tested on our dataset consisting of 169 known and 8 unknown vehicles. We use stratified k-fold cross validation with $k = 10$ to evaluate our approach. The resulting confusion matrix is shown in Table IV. All sedans are correctly classified except for the one which is misclassified as a pickup truck [see Fig. 13(a)]. Fig. 13(b) shows an SUV misclassified as a pickup truck. A closer look at the data and pattern-feature matrix shows great similarity for both these cases with the pickup class due to the license plate location and rear tail light width.

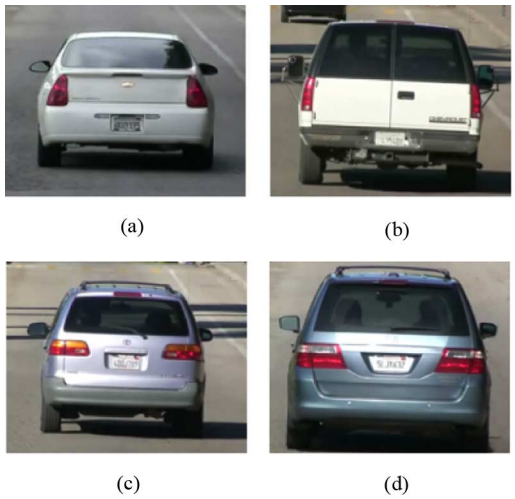

(a) (b) (c) (d)

Fig. 13. Misclassified examples. (a) Sedan misclassified as pickup. (b) SUV misclassified as pickup. (c) Minivan misclassified as sedan. (d) Minivan misclassified as sedan.

TABLE V
STRUCTURE LEARNING EVALUATION

Structure Learning Method	Precision	FA Rate	CCR
K2 algorithm & BIC (Figure 8(a))	93.68	0.04	96.06
Manual chosen structure (Figure 8(b))	95.68	0.02	97.63

TABLE VI
CCR COMPARISON FOR KNN, LDA, SVM, AND HDBN

Classifier→ Vehicle Class↓	kNN	LDA	SVM	HDBN
Sedan	88.25	94.67	96.44	97.63
Pickup	95.12	94.67	96.44	98.22
SUV/Minivan	90.90	92.89	92.30	97.04
Overall	91.42	94.07	95.06	97.63

E. Structure Learning Evaluation

Table V presents the classification evaluation metrics for the two structures given in Fig. 8(a) and 8(b). The results show that learning the structure using K2 decreases the classification accuracy and precision. This is due to the fact that the K2 search algorithm requires a known linear ordering of nodes prior to model selection. One way to overcome this is to determine the ordering of nodes prior to performing K2. Determining the required ordering using a dynamic programming approach takes $O(n^2 2^n)$ time and $O(n2^n)$ space, where n is the number of nodes. The linear order determines the possible parent candidates for each node in a way that the BN is guaranteed to be an acyclic graph.

F. Comparison With Other Methods

We compare our results with three well-known classifiers: k-nearest neighbor (kNN), linear discriminant analysis (LDA), and SVM. All classification algorithms use the same feature set as the HDBN classifier. Tables VI–VIII show classification accuracy, false positive ratio (false alarm), and precision respectively. The class "unknown" is not included in computing the results for Tables VI–VIII.

TABLE VII
FALSE ALARM PERCENTAGES COMPARISON

Classifier→ Vehicle Class↓	kNN	LDA	SVM	HDBN
Sedan	0.17	0.07	0.06	0.04
Pickup	0.04	0.05	0.03	0.02
SUV/Minivan	0.04	0.02	0.04	0
Overall	0.09	0.05	0.04	0.02

TABLE VIII
PRECISION PERCENTAGES COMPARISON

Classifier→ Vehicle Class↓	kNN	LDA	SVM	HDBN
Sedan	88.46	95.05	96.07	97.05
Pickup	80.64	78.13	86.20	90.00
SUV/Minivan	85.29	91.67	87.17	100
Overall	84.80	88.28	89.81	95.68

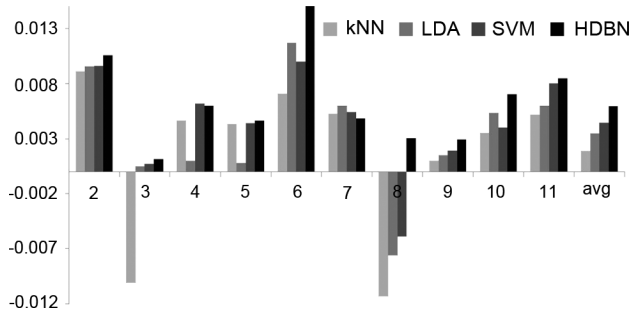

Fig. 14. Feature CCR contribution comparison.

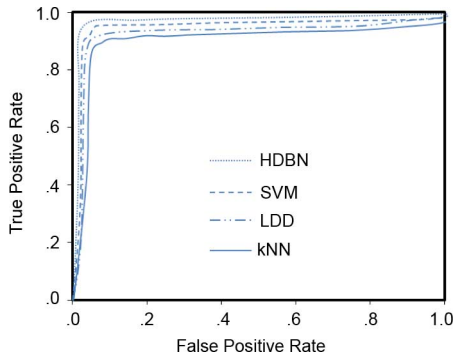

Fig. 15. Performance ROC plot.

Fig. 14 demonstrates how each feature individually contributes to the CCR for all four classifiers kNN, LDA, SVM, and the proposed HDBN. Each bar indicates how much on average the corresponding feature increases/decrease the CCR. The experiment shows that when using HDBN, every feature has a positive contribution, whereas for the other three classifiers, particular features may decrease the CCR (e.g., feature for kNN, feature 8 for kNN, LDA, and SVM). This observing shows that HDDN is more tolerant to unreliable/noisy features than the other classifiers discussed here. Another interesting fact is related to each classifiers performance on the features. On our dataset, HDBN tends to be a more accurate classifier when features are not linearly separable (e.g., feature 8).

Fig. 15 presents the receiver operating characteristic (ROC) curves for all the four classifiers. Although the ROC curves are similar, it is clear that HDBN out performs SVM, LDA, and KNN.

V. CONCLUSION

We proposed a DBN for vehicle classification and showed that using multiple video frames in a DBN structure can outperform well-known classifiers such as kNN, LDA, and SVM. Our experiments showed that obtaining high classification accuracy does not always require high-level features and simple features (e.g., normalized distance and angle) may also provide such results making it possible to perform real-time classification. Future work will involve converting the current training-testing model to an incremental online learning model, stochastic vehicle make and model identification, and adaptive DBN structure learning for classification purposes.

REFERENCES

[1] Y. Shan, H. Sawhney, and R. Kumar, "Unsupervised learning of discriminative edge measures for vehicle matching between nonoverlapping cameras," *IEEE Trans. Pattern Anal. Mach. Intell.*, vol. 30, no. 4, pp. 700–711, Apr. 2008.

[2] T. Lim and A. Guntoro, "Car recognition using Gabor filter feature extraction," in *Proc. Asia-Pacif. Conf. Circuits Syst.*, 2002, vol. 2, pp. 451–455.

[3] W. Wu, Z. QiSen, and W. Mingjun, "A method of vehicle classification using models and neural networks," in *Proc. IEEE VTS 53rd Veh. Technol. Conf.*, 2001, vol. 4, pp. 3022–3026.

[4] X. Ma and W. Grimson, "Edge-based rich representation for vehicle classification," in *Proc. 10th IEEE Int. Conf. Comput. Vis.*, Oct. 2005, vol. 2, pp. 1185–1192.

[5] M.-P. D. Jolly, S. Lakshmanan, and A. Jain, "Vehicle segmentation and classification using deformable templates," *IEEE Trans. Pattern Anal. Mach. Intell.*, vol. 18, no. 3, pp. 293–308, Mar. 1996.

[6] S. Khan, H. Cheng, D. Matthies, and H. Sawhney, "3D model based vehicle classification in aerial imagery," in *Proc. IEEE Conf. Comput. Vis. Pattern Recognit.*, Jun. 2010, pp. 1681–1687.

[7] J. Prokaj and G. Medioni, "3D model based vehicle recognition," in *Proc. Workshop Appl. Comput. Vis.*, 2009, pp. 1–7.

[8] J. Wu and X. Zhang, "A PCA classifier and its application in vehicle detection," in *Proc. Int. Joint Conf. Neural Netw.*, 2001, vol. 1, pp. 600–604.

[9] M. Conos, "Recognition of vehicle make from a frontal view," Master thesis, Czech Tech. Univ., Prague, Czech Republic, 2006.

[10] A. Psyllos, C. N. Anagnostopoulos, and E. Kayafas, "Vehicle model recognition from frontal view image measurements," *Comput. Standard Interfaces*, vol. 33, pp. 142–151, Feb. 2011.

[11] L. Dlagnekov and S. Belongie, Recognizing cars Univ. California, San Diego, CA, Tech. Rep. CS2005-083, 2005.

[12] Z. Chen, N. Pears, M. Freeman, and J. Austin, "Road vehicle classification using support vector machines," in *Proc. IEEE Int. Conf. Intell. Comput. Intell. Syst.*, Nov. 2009, vol. 4, pp. 214–218.

[13] D. Zhang, S. Qu, and Z. Liu, "Robust classification of vehicle based on fusion of TSRP and wavelet fractal signature," in *Proc. IEEE Conf. Netw., Sens. Control*, 2008, pp. 1788–1793.

[14] Y.-L. Chen, B.-F. Wu, H.-Y. Huang, and C.-J. Fan, "A real-time vision system for nighttime vehicle detection and traffic surveillance," *IEEE Trans. Ind. Electron.*, vol. 58, no. 5, pp. 2030–2044, May 2011.

[15] X. Cao, C. Wu, J. Lan, P. Yan, and X. Li, "Vehicle detection and motion analysis in low-altitude airborne video under urban environment," *IEEE Trans. Circuits Syst. Video Technol.*, vol. 21, no. 10, pp. 1522–1533, Oct. 2011.

[16] F. Alves, M. Ferreira, and C. Santos, "Vision based automatic traffic condition interpretation," in *Proc. 8th IEEE Int. Conf. Ind. Informat.*, Jul. 2010, pp. 549–556.

[17] M. Chacon and S. Gonzalez, "An adaptive neural-fuzzy approach for object detection in dynamic backgrounds for surveillance systems," *IEEE Trans. Ind. Electron.*, Accepted for publication, Dec. 29, 2010.

[18] S. Nadimi and B. Bhanu, "Multistrategy fusion using mixture model for moving object detection," in *Proc. Int. Conf. Multisens. Fusion Integr. Intell. Syst.*, 2001, pp. 317–322.

[19] G. Loy and J. O. Eklundh, "Detecting symmetry and symmetric constellations of features," in *Proc. Eur. Conf. Comput. Vis.*, 2006, pp. 508–521.
[20] S. Nadimi and B. Bhanu, "Physical models for moving shadow and object detection in video," *IEEE Trans. Pattern Anal. Mach. Intell.*, vol. 26, no. 8, pp. 1079–1087, 2004.
[21] W.-Y. Ho and C.-M. Pun, "A macao license plate recognition system based on edge and projection analysis," in *Proc. 8th IEEE Int. Conf. Ind. Informat.*, Jul. 2010, pp. 67–72.
[22] C. Anagnostopoulos, I. Anagnostopoulos, V. Loumos, and E. Kayafas, "A license plate-recognition algorithm for intelligent transportation system applications," *IEEE Trans. Intell. Transp. Syst.*, vol. 7, no. 3, pp. 377–392, Sep. 2006.
[23] V. Abolghasemi and A. Ahmadyfard, "An edge-based color-aided method for license plate detection," *Image Vision Comput.*, vol. 27, pp. 1134–1142, Jul. 2009.
[24] C. Paulo and P. Correia, "Automatic detection and classification of traffic signs," in *Proc. 8th Int. Workshop Image Anal. Multimedia Interactive Services*, Jun. 2007, p. 11.
[25] Y. Guo, C. Rao, S. Samarasekera, J. Kim, R. Kumar, and H. Sawhney, "Matching vehicles under large pose transformations using approximate 3D models and piecewise MRF model," in *Proc. IEEE Conf. Comput. Vis. Pattern Recognit.*, 2008, pp. 1–8.
[26] N. Otsu, "A threshold selection method from gray-level histograms," *IEEE Trans. Syst., Man, Cybern.*, vol. 9, no. 1, pp. 62–66, Jan. 1979.
[27] H. Sakoe and S. Chiba, "Dynamic programming algorithm optimization for spoken word recognition," *IEEE Trans. Acoust., Speech Signal Process.*, vol. 26, no. 1, pp. 43–49, Feb. 1978.
[28] K. P. Murphy, "The Bayes net toolbox for MATLAB," in *Comput. Sci. Statist.: Proc. Interface*, 2001, vol. 33 [Online]. Available: http://code.google.com/p/bnt/, Online. Available:

Mehran Kafai (S'11) received the B.S. degree in computer engineering from Bahonar University, Kerman, Iran, in 2002, the M.S. degree in computer engineering from the Sharif University of Technology, Tehran, Iran, in 2005, and the M.S. degree in computer science from the San Francisco State University, San Francisco, CA, in 2009. He is currently working toward the Ph.D. degree in computer science at the Center for Research in Intelligent Systems, University of California, Riverside.

His research interests include computer vision, pattern recognition, machine learning, and data mining. His recent research has been concerned with robust object recognition algorithms.

Bir Bhanu (S'72–M'82–SM'87–F'95) received the S.M. and E.E. degrees in electrical engineering and computer science from the Massachusetts Institute of Technology, Cambridge, the Ph.D. degree in electrical engineering from the Image Processing Institute, University of Southern California, Los Angeles, and the M.B.A. degree from the University of California, Irvine.

He is the Distinguished Professor of Electrical Engineering and serves as the Founding Director of the Interdisciplinary Center for Research in Intelligent Systems, University of California, Riverside (UCR). He was the founding Professor of Electrical Engineering at UCR and served as its First Chair during 1991–1994. He has been the cooperative Professor of Computer Science and Engineering (since 1991), Bioengineering (since 2006), Mechanical Engineering (since 2008), and the Director of Visualization and Intelligent Systems Laboratory (since 1991). Previously, he was a Senior Honeywell Fellow with Honeywell Inc., Minneapolis, MN. He has been with the faculty of the Department of Computer Science, University of Utah, Salt Lake City, and with Ford Aerospace and Communications Corporation, Newport Beach, CA; INRIA-France; and IBM San Jose Research Laboratory, San Jose, CA. He has been the principal investigator of various programs for the National Science Foundation, the Defense Advanced Research Projects Agency (DARPA), the National Aeronautics and Space Administration, the Air Force Office of Scientific Research, the Office of Naval Research, the Army Research Office, and other agencies and industries in the areas of video networks, video understanding, video bioinformatics, learning and vision, image understanding, pattern recognition, target recognition, biometrics, autonomous navigation, image databases, and machine-vision applications. He is the coauthor of the books *Computational Learning for Adaptive Computer Vision* (Forthcoming), *Human Recognition at a Distance in Video* (Berlin, Germany: Springer-Verlag, 2011), *Human Ear Recognition by Computer* (Berlin, Germany: Springer-Verlag, 2008), *Evolutionary Synthesis of Pattern Recognition Systems* (Berlin, Germany: Springer-Verlag, 2005), *Computational Algorithms for Fingerprint Recognition* (Norwell, MA: Kluwer, 2004), *Genetic Learning for Adaptive Image Segmentation* (Norwell, MA: Kluwer, 1994), and *Qualitative Motion Understanding* (Norwell, MA: Kluwer, 1992), and coeditor of *Computer Vision Beyond the Visible Spectrum* (Berlin, Germany: Springer-Verlag, 2004), *Distributed Video Sensor Networks* (Berlin, Germany: Springer-Verlag, 2011), and *Multibiometrics for Human Identification* (Cambridge, U.K.: Cambridge Univ. Press, 2011). He is the holder of 18 (5 pending) U.S. and international patents. He has more than 350 reviewed technical publications, including more than 100 journal papers.

Dr. Bhanu has been on the Editorial Board of various journals and has edited special issues of several IEEE Transactions (IEEE TRANSACTIONS ON PATTERN ANALYSIS AND MACHINE INTELLIGENCE, the IEEE TRANSACTIONS ON IMAGE PROCESSING, the IEEE TRANSACTIONS ON SYSTEMS, MAN, AND CYBERNETICS—PART B: CYBERNETICS, the IEEE TRANSACTIONS ON ROBOTICS AND AUTOMATION, and the IEEE TRANSACTIONS ON INFORMATION FORENSICS SECURITY) and many other journals. He was the General Chair for the IEEE Conference on Computer Vision and Pattern Recognition, the IEEE Conference on Advanced Video and Signal-Based Surveillance, the IEEE Workshops on Applications of Computer Vision, the IEEE Workshops on Learning in Computer Vision and Pattern Recognition; the Chair for the DARPA Image Understanding Workshop, the IEEE Workshops on Computer Vision Beyond the Visible Spectrum, and the IEEE Workshops on Multi-Modal Biometrics. He

Dr. Bhanu was the recipient of Best Conference Papers and Outstanding Journal Paper Awards and the Industrial and University Awards for Research Excellence, Outstanding Contributions, Team Efforts and Doctoral/Dissertation Advisor/Mentor Award. He is a Fellow of the American Association for the Advancement of Science, the International Association of Pattern Recognition, and the International Society for Optical Engineering.